

Rapid imaging of gravity gradiometry data using 2D potential field migration

Michael S. Zhdanov*, The University of Utah and TechnoImaging, Xiaojun Liu, The University of Utah, and Glenn A. Wilson, TechnoImaging

Summary

We introduce 2D potential field migration for the interpretation of gravity gradiometry data. This method is based on a direct integral transformation of the observed gravity gradients into subsurface density distributions which can be used for real-time imaging or as an a priori model for subsequent 3D regularized inversion. Potential field migration is very fast and stable with respect to noise, as it reduces the downward continuation of the migration field to a well-behaved analytic function everywhere in the subsurface. Hence, potential field migration avoids the numerical instabilities of the other imaging methods based on conventional downward continuation. We present a case study for the interpretation of gravity gradiometry data acquired in the Nordkapp Basin in the Norwegian sector of the Barents Sea. We observe agreement with results obtained from potential field migration with those obtained from 3D regularized inversion.

Introduction

Gravity gradiometry has come to be routinely integrated in exploration workflows since it can provide an independent measure of the subsurface density distribution. The advantage of gravity gradiometry over other gravity methods is that the data are extremely sensitive to localized density contrasts within regional geological settings. Moreover, high quality data can now be acquired over very large areas for relatively low cost from either air- or ship-borne platforms. This makes the method ideally suited to delineating salt structures, and for detecting kimberlite pipes. The interpretation of gravity gradiometry data using 3D regularized inversion has been discussed in a number of publications (e.g., Li, 2001; Zhdanov et al., 2004). A variety of fast imaging techniques related to Euler decomposition have also been developed; most of which are based on the superposition of analytical responses from specific sources. These imaging methods estimate the positions and some parameters of the sources based on field attenuation characteristics. In this paper, we develop a different approach to imaging; one which we base on the idea of potential field migration as originally introduced by Zhdanov (2002). The concept of the migration was developed for seismic wave fields (e.g., Schneider, 1978; Berkhout, 1980; Claerbout, 1985). It has since been demonstrated that this concept could also be extended to electromagnetic and potential fields (Zhdanov, 1988, 2002, 2009). Potential field migration is based on a special form of downward continuation of the potential field or one of its gradients. This downward continuation is obtained as the solution of the boundary value problem to Laplace's equation in the lower half-space, in which the boundary values of the migration field on the Earth's

surface are determined from the observed data. It is important to stress that potential field migration is not the same as analytic continuation because it transforms the observed field into a migration field, and does not attempt to reconstruct the true potential field. However, the migration field does contain remnant information about the original source distribution which is why it can be used for subsurface imaging.

2D potential field migration of gravity fields and their gradients

For a 2D gravity field, we can define the complex intensity:

$$g(\zeta) = -g_x(x, z) + i g_z(x, z),$$

where $\zeta = x + iz$ is a complex coordinate of the point (x, z) in the vertical plane. This satisfies the equation:

$$g(\zeta') = A_g(\rho) = -2\gamma \iint_{\Gamma} \frac{1}{\zeta - \zeta'} \rho(\zeta) ds,$$

where $\rho(\zeta) = \rho(x, z)$ and $A_g(\rho)$ denotes the forward operator for the gravity field. We can introduce the adjoint operator of the gravity field applied to a complex function $f(\zeta')$:

$$A_g^*(f) = 2\gamma \int_{-\infty}^{\infty} \frac{f^*(x')}{x' - \zeta} dx'.$$

Similarly, for the gravity gradients we can define the complex intensity as a complex derivative of the complex intensity of the gravity field:

$$g_T(\zeta) = -g_{xx}(x, z) + i g_{zx}(x, z),$$

where we have taken into account the symmetry of the gravity gradients. The complex intensity of the gravity gradients can be found based on the equation:

$$g_T(\zeta') = A_T(\rho) = -2\gamma \iint_{\Gamma} \frac{1}{(\zeta - \zeta')^2} \rho(\zeta) ds,$$

where $A_T(\rho)$ denotes the forward operator of the gravity gradients. We can introduce the adjoint operator of the gravity gradients applied to a complex function $f(\zeta')$:

$$A_T^*(f) = -2\gamma \int_L \frac{f^*(\zeta')}{(\zeta - \zeta')^2} d\zeta'.$$

Rapid imaging of gravity gradiometry data using 2D potential field migration

The potential field migration of gravity fields was first described by Zhdanov (2002), and was introduced as the application of the adjoint gravity operator to the complex intensity of the observed gravity field:

$$g_g^m(\zeta) = \frac{i}{4\pi\gamma} A_g^* g_g(\zeta).$$

If the profile of observed gravity fields coincides with the horizontal axis, then the actions of the adjoint gravity operator are equivalent to analytical continuation of the complex conjugate of the observed gravity fields in the lower half-space. Similarly, the adjoint gravity gradient operator is equivalent to the derivative of the analytic continuation of the complex conjugate of the observed gravity gradients in the lower half-space:

$$g_T^m(\zeta) = \frac{\partial}{\partial \zeta} g_T^*(\zeta) = \frac{i}{4\pi\gamma} A_T^* g_T(\zeta).$$

Migration of the gravity gradients involves an additional differential operation, while migration of gravity fields requires analytic continuation only. From a physical point of view, the migration fields are obtained by moving the sources of the observed fields above their profile. The migration fields contain remnant information about the original sources of the gravity fields and their gradients, and thus can be used for subsurface imaging. There is a significant difference between conventional downward analytical continuation and migration of the observed gravity fields and their gradients. The observed gravity fields and their gradients have singular points in the lower half-space associated with their sources. Hence, analytic continuation is an ill-posed and unstable transformation as the gravity fields and their gradients can only be continued down to these singularities (Strakhov, 1970; Zhdanov, 1988). On the contrary, the migration fields are analytic everywhere in the lower half-space, and migration itself is a well-posed, stable transformation. However, direct application of adjoint operators to the observed gravity fields and their gradients does not produce adequate images of the density distributions. In order to image the sources of the gravity fields and their gradients at the correct depths, an appropriate spatial weighting operator needs to be applied to the migration fields. For the gravity migration field, we can derive the *gravity migration density*:

$$\rho_T^m(\zeta) = -4\pi\gamma k_T w_T^{-2}(z) \text{Re}[i g_T^m(\zeta)],$$

which is proportional to the weighted real part of the gravity migration field, where k_g is a scalar function and the weighting function w_g is proportional to the integrated sensitivity of the gravity fields (Zhdanov, 2002). Thus, the migration transformation with spatial weighting provides a stable algorithm for evaluating the gravity migration density.

Likewise for the gravity gradients, we can derive the *gravity gradient migration density*:

$$\rho_T^m(\zeta) = -4\pi\gamma k_T w_T^{-2}(z) \text{Re}[i g_T^m(\zeta)],$$

which is proportional to the weighted real part of the gravity migration field. Figure 1 presents the gravity migration density from a profile above a point source. It is clear that the maximum of the gravity migration density is located at the position of the source. In Figure 2, we present the gravity gradient migration density from a profile above the same point source. Again, one can see that the maximum of the gravity gradient migration density is located at the position of the source. Moreover, migration of the gravity gradient data provides a more focused image than migration of the gravity data. This fact indicates that gravity gradient migration can provide better images of localized subsurface structures than gravity migration.

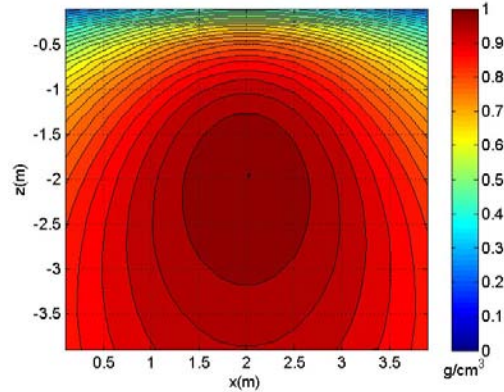


Figure 1. Gravity migration density for a point source located at (2,-2).

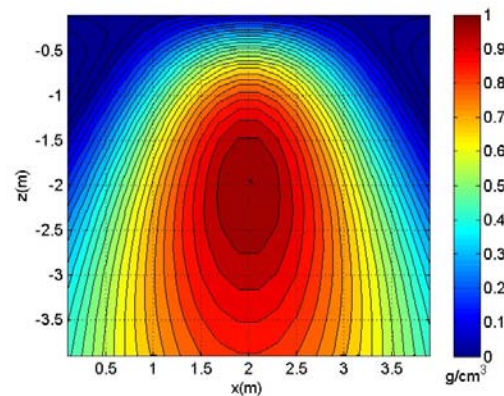


Figure 2. Gravity gradient migration density for a point source located at (2,-2).

Rapid imaging of gravity gradiometry data using 2D potential field migration

Model study

We consider an along strike profile above two long rectangular prisms with a density of 1 g/cm^3 located 100 m below the profile, as shown in the middle panel of Figure 3. With no noise added to the data, the gravity gradient migration density is shown in the lower panel of Figure 3, along with the outlines of the two prisms.

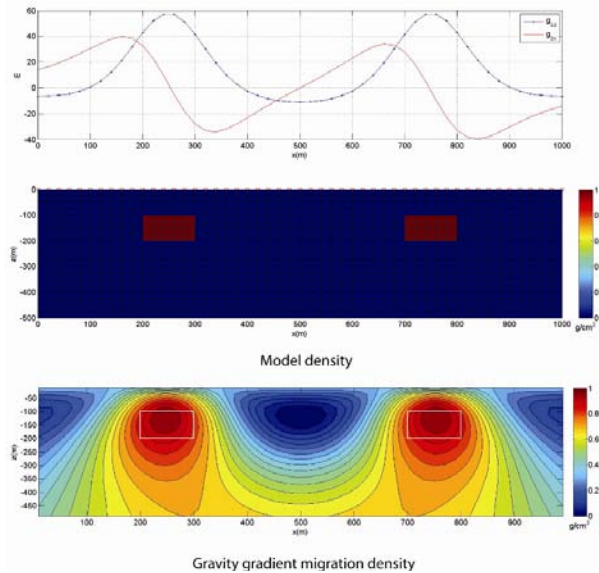


Figure 3. The top panel shows profiles of the gravity gradient components $g_{zz}(x, 0)$ and $g_{zx}(x, 0)$ along strike of two long prisms. The middle panel shows a vertical section of the model density distribution. The lower panel shows the gravity gradient migration density.

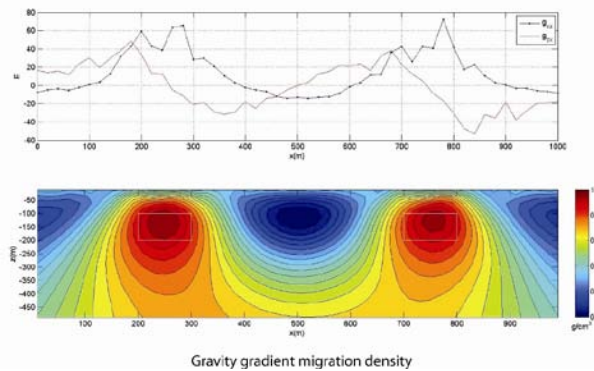


Figure 4. The top panel shows profiles of the gravity gradient components $g_{zz}(x, 0)$ and $g_{zx}(x, 0)$ along strike of two long prisms with 10% random Gaussian noise added. The lower panel shows the gravity gradient migration density.

We then added 10% random Gaussian noise to the data, as shown in the top panel of Figure 4. The gravity gradient migration density is shown in the lower panel of Figure 4, along with the outlines of the two prisms. Clearly, the gravity gradient migration method is very resilient, and can provide high quality images of the density distribution for noisy data.

Case study – Nordkapp Basin

The Nordkapp Basin is located in the Norwegian sector of the Barents Sea, and is an intra-continental salt basin containing over 30 salt structures. The salt is of an Early Permian age, and was mobilized by Early Triassic sedimentation. Tertiary uplift and erosion removed nearly 1400 m of Cretaceous and younger sediments (Neilsen et al., 1995). The petroleum plays are mainly salt-related traps. Only two wells have been drilled in the basin; the Pandora well which was a discovery, and the Uranus well which terminated inside salt. Recent discoveries in other nearby basins suggest potential for further hydrocarbon discoveries within the Nordkapp Basin (Hokstad et al., 2009). Improved seismic imaging changed the structural interpretations of the salt diapirs from what were initially thought of as wide salt stocks with vertical flanks to more complex geometries with broad diapirs overhanging narrow stems. Much of the exploration risk associated with these structures results from distortions in the seismic imaging, and subsequent ambiguity of the salt isopach.

A full tensor gradient (FTG) survey was acquired over the Nordkapp Basin with the intent of delineating salt geometry. The Tertiary rocks in the area have a density between 2.30 and 2.38 g/cm^3 . The salt diapirs are characterized by negative density contrasts relative to the surrounding sediments and thus can be identified from the gravity gradiometry data. In this paper, we focus on results for the Obelix prospect in the southwest of the basin; particularly the G2, F1 and F2 salt diapirs shown in Figure 5. We performed 2D migration along nine profiles of g_{zz} and g_{zx} data so as to obtain 2D images of the density distributions, shown in Figure 6. For comparison, we show the same cross-sections obtained from 3D regularized inversion in Figure 7 (Wan and Zhdanov, 2008). We can see the same typical negative density contrasts in both of these figures. Figure 8 is the 2D gravity migration along profile A-A'. This is co-rendered with the corresponding seismic depth migration image. Salt diapir F2 is clearly identified in both the gravity and seismic migration images.

Rapid imaging of gravity gradiometry data using 2D potential field migration

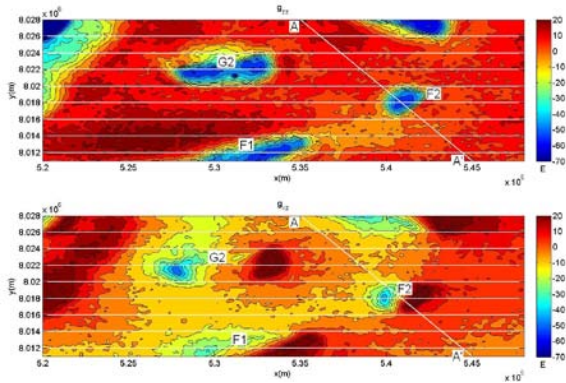


Figure 5. g_{zz} and g_{xz} survey data for the Obelix prospect in the Nordkapp Basin. Salt diapirs G2, F1 and F2 are shown. Profile lines are also marked in white.

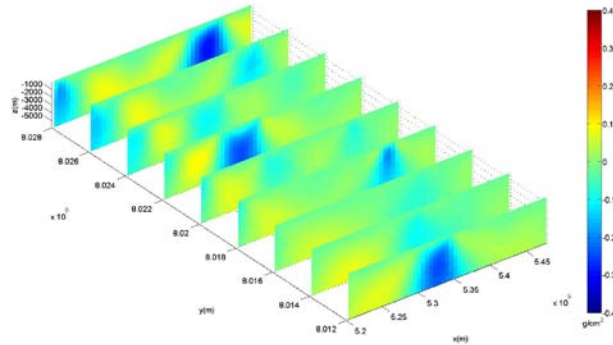


Figure 6. 2D vertical cross-sections of density contrasts in the Nordkapp Basin obtained from 2D gravity migration of each profile.

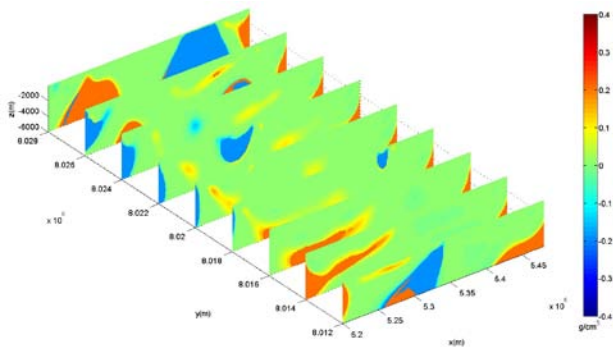


Figure 7. 2D vertical cross-sections of density contrasts in the Nordkapp Basin obtained from 3D regularized inversion with focusing (from Wan and Zhdanov, 2008).

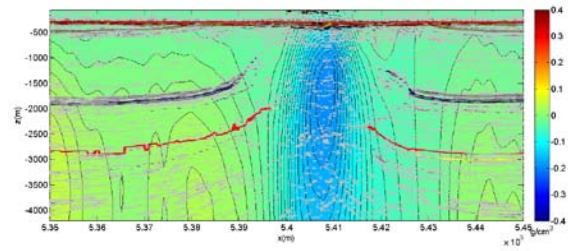


Figure 8. 2D gravity migration image along profile A-A' co-rendered with the corresponding seismic depth migration image.

Conclusions

We have introduced a new method for interpreting gravity gradiometry data based on potential field migration. The method is based on an integral transformation of gravity gradiometry data into an image of subsurface density distributions. Potential field migration is fast and stable, and can be used for real-time imaging or for preparing an a priori model for subsequent 3D regularized inversion. Currently, the method is implemented for the migration of 2D profiles of gravity and gravity gradiometry data. We have demonstrated this with a case study for salt mapping from the Nordkapp Basin in the Barents Sea. The method can be naturally extended to 3D, as well as to magnetic fields and their gradients. This constitutes our future research activities.

Acknowledgements

The authors acknowledge TechnoImaging for support of this research and permission to publish. Dr. Brian Farrelly and StatoilHydro are acknowledged for providing the Barents Sea gravity gradiometry data, and for their permission to publish. Zhdanov and Liu acknowledge the support of The University of Utah's Consortium for Electromagnetic Modeling and Inversion (CEMI).

EDITED REFERENCES

Note: This reference list is a copy-edited version of the reference list submitted by the author. Reference lists for the 2010 SEG Technical Program Expanded Abstracts have been copy edited so that references provided with the online metadata for each paper will achieve a high degree of linking to cited sources that appear on the Web.

REFERENCES

- Berkhout, A. J., 1980, *Seismic migration*: Elsevier.
- Claerbout, J. F., 1985, *Imaging the Earth's interior*: Blackwell.
- Hokstad, K., E. A. Myrland, and B. Fotland, 2009, Salt imaging in the Nordkapp Basin with electromagnetic data: Presented at AAPG 3-P Arctic Conference and Exhibition.
- Li, Y., 2001, 3D inversion of gravity gradiometer data: 71st Annual International Meeting, SEG, Expanded Abstracts, 1470-1473.
- Nielsen, K. T., B. C. Vendeville, and J. T. Johansen, 1995, Influence of regional tectonics on halokinesis in the Norkapp Basin, Barents Sea: *AAPG Memoir*, **65**, 413–436.
- Schneider, W. A., 1978, Integral formulation for migration in two and three dimensions: *Geophysics*, **43**, 49–76, [doi:10.1190/1.1440828](https://doi.org/10.1190/1.1440828).
- Strakhov, V. N., 1970, Some aspects of the plane gravitational problem (in Russian): *Izvestiya Akademi Nauk SSSR Fizika Zemli*, **12**, 32–44.
- Wan, L., and M. S. Zhdanov, 2008, Focusing inversion of marine full-tensor gradiometry data in offshore geophysical exploration: 78th Annual International Meeting, SEG, Expanded Abstracts, 751-754.
- Zhdanov, M. S., 1988, *Integral Transforms in Geophysics*: Springer-Verlag.
- Zhdanov, M. S., 2002, *Geophysical Inverse Theory and Regularization Problems*: Elsevier.
- Zhdanov, M. S., 2009, *Geophysical Electromagnetic Theory and Methods*: Elsevier.